Synthesis and Preliminary Biological Evaluation of Indol-3-yl-oxoacetamides as Potent Cannabinoid Receptor Type 2 Ligands

Rareş-Petru Moldovan [1,*], Winnie Deuther-Conrad [1], Andrew G. Horti [2] and Peter Brust [1]

[1]   Helmholtz-Zentrum Dresden-Rossendorf e.V., Institute of Radiopharmaceutical Cancer Research, Permoserstr. 15, 04318 Leipzig, Germany; w.deuther-conrad@hzdr.de (W.D.-C.); p.brust@hzdr.de (P.B.)
[2]   Johns Hopkins School of Medicine, Division of Nuclear Medicine and Molecular Imaging, Department of Radiology, Baltimore, MD 21287, USA; ahorti1@jhmi.edu
[*]   Correspondence: r.moldovan@hzdr.de; Tel.: +49-341-234-179-4634

Abstract: A small series of indol-3-yl-oxoacetamides was synthesized starting from the literature known *N*-(adamantan-1-yl)-2-(5-(furan-2-yl)-1-pentyl-1*H*-indol-3-yl)-2-oxoacetamide (**5**) by substituting the 1-pentyl-1*H*-indole subunit. Our preliminary biological evaluation showed that the fluorinated derivative 8 is a potent and selective CB_2 ligand with K_i = 6.2 nM.

1. Introduction

For centuries, *Cannabis sativa* was used as medicinal plant for the treatment of pain and inflammatory processes. The discovery by Gaoni and Mechoulam [1] of Δ^9-tetrahydrocannabinol (Δ^9-THC)—the primary psychoactive ingredient in *Cannabis sativa*—set the stage for the identification of the endogenous cannabinoid (endocannabinoid) transmitter system in the brain. The endocannabinoid system consists of cannabinoid (CB) receptors, endogenous ligands (e.g., anandamide, 2-*O*-arachidonoylglycerol) that activate the CB receptors, and the enzymes, which are responsible for the biosynthesis (e.g., *N*-acyltransferase, diacylglycerol lipase) and deactivation (e.g., fatty acid amide hydrolases, monoacylglycerol lipases) of the endogenous ligands [2,3].

Two types of specific $G_{i/o}$-protein-coupled CB receptors were cloned in the 1990s, termed CB_1 and CB_2 receptor [4,5]. CB_1 receptors are abundantly expressed in the central nervous system, and their function has been thoroughly investigated [6]. Recently, the crystal structure of the CB_1 receptors has been reported, providing a tool for a more accurate pharmacological investigation of this receptor subtype [7,8]. In contrast to CB_1 receptors, the CB_2 receptor was originally regarded as a peripheral receptor predominantly expressed in cells of the immune system [5,9,10]. However, more recent investigations proved the presence of CB_2 receptors in glial cells (microglia and astrocytes) [11,12], and oligodendroglial [13] progenitors in vitro, as well as in microglia [14] and neuronal progenitors [12] in normal mouse brain in vivo [15].

The predominant expression of the CB_2 receptor in cells of the immune system suggests a modulation of diverse immune functions, including cytokine production, lymphocyte proliferation, and humoral and cell-mediated immune responses [16,17]. With respect to neuroinflammation, microglia adopt a key function. Under healthy conditions, the expression of CB_2 receptors in the brain is rather low [18]. However, inflammatory effects result in considerably increased expression levels of CB_2 receptors [19,20]. It was found that neurodegenerative and neuroinflammatory processes in the brain related to, for example, depression, Alzheimer's disease, multiple sclerosis, amyotrophic

lateral sclerosis, or brain tumors such as glioblastoma are associated with an upregulation of CB_2 receptor expression [18,21–23]. CB_2 receptor agonists lead to a reduction of neuroinflammation and stimulation of neurogenesis. Therefore, the therapeutic potential of CB_2 agonists is related to neurodegenerative and neuroinflammatory processes [19,24]. Moreover, the availability of CB_2 receptors as measured with positron emission tomography (PET) [25] could potentially be used as a biomarker for neurodegenerative and neuroinflammatory processes in the brain [26–29].

Indole has been a very popular key building block for the medicinal chemistry of cannabinoid receptor ligands, and a large number of indole-derived CB_2 selective ligands have been developed [30–33]. However, most of these ligands do not comply with the most important needs of a ligand suitable for the development of a tracer for CB_2 brain imaging with PET; namely, high affinity towards CB_2 ($K_i(CB_2) < 1$ nM) and high selectivity over CB_1 ($K_i(CB_2)/(CB_1)$ > 500) [26,34]. Recently, we reported the development of a highly affine and selective ^{18}F-labeled CB_2 radiotracer ($K_i(CB_2) = 0.4$ nM, $K_i(CB_1) = 380$ nM), and proved its applicability in a mouse model of neuroinflammation [35]. However, this radioligand suffers from low metabolic stability in vivo, and therefore we redirected our focus on the structure of the literature known, highly affine *N*-(adamantan-1-yl)-2-(5-(furan-2-yl)-1-pentyl-1*H*-indol-3-yl)-2-oxoacetamide (**5**, $K_i(CB_2) = 0.37$ nM and $K_i(CB_1) = 345$ nM) [32] for the development of a CB_2 radiotracer. In the present work, we show the synthesis and preliminary biological evaluation of fluorine-containing indol-3-yl-oxoacetamide derivatives.

2. Results and Discussion

The structure–affinity relationship study which lead to the identification of compound **5** [32,36] (Scheme 1) and the work performed on the structurally related quinolinone-3-carboxamides as CB_2 ligands [37] has proven the importance of the substitution pattern at the 5-indole position, and also the need of the lipophilic adamantane subunit. Herein, we investigate the possibility of introducing a fluorine atom by modifying the alkyl chain at the indole 1-position.
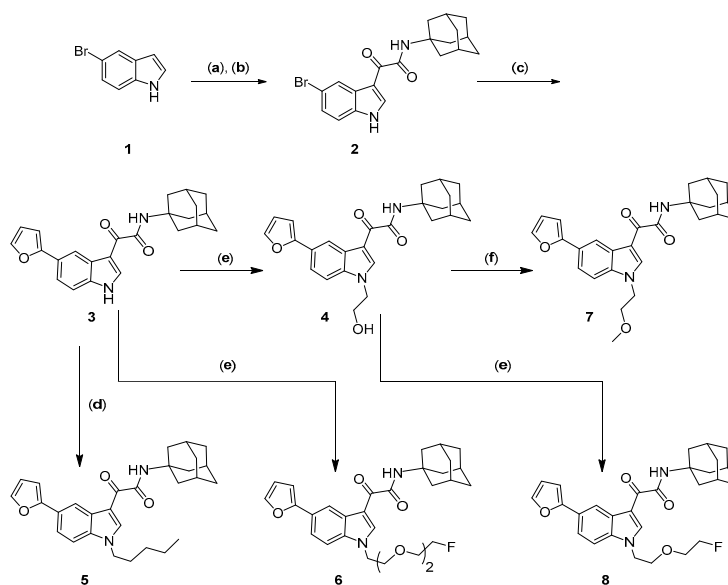
Scheme 1. Synthesis of the key building block **3**, lead compound **5**, and ether derivatives **6**, **7**, and **8**; (**a**) oxalyl chloride, diethyl ether (Et$_2$O), 0 °C to r.t., 1.5 h, 60%; (**b**) amantadine, triethylamine (Et$_3$N), dichloromethane (DCM), r.t., 16 h, 82%; (**c**) 2-furanboronic acid, tetrakis(triphenylphosphine)palladium(0) (Pd(PPh$_3$)$_4$), Na$_2$CO$_3$, EtOH, reflux, 14 h, 60%; (**d**) 1-bromobutane (*n*-BuBr), tetrabutylammonium bromide (TBAB), 20% aq. NaOH, DCM, r.t., 14 h, 72%; (**e**) bromo-alkyl reagent, KOH, *N*,*N*-dimethylformamide (DMF), 90 °C, 6 h, 67%–72%; (**f**) NaH, methyl iodide (MeI) for **7** and Br(CH$_2$)$_2$F for **8**, DMF, 0 °C to r.t., 6 h, 85%–90% [32].

The synthesis of the key building block **3** was performed as described in the literature [32] and depicted in Scheme 1. Treatment of 5-bromoindole (**1**) with oxalyl chloride delivered the corresponding indole-3-oxoacetyl chloride in ~60% yield, which was further reacted with amantadine (adamantan-1-amine) in presence of triethylamine (Et$_3$N) to give compound **2**. Next, Suzuki coupling was performed using the commercially available 2-furanboronic acid in presence of Pd(PPh$_3$)$_4$ and Na$_2$CO$_3$ to give **3**. The lead molecule **5** [32] was synthesized by treating **3** with 1-bromobutane in basic reaction condition in ~25% yield over four steps starting from **1**, as a light yellow solid. To overcome the high lipophilicity of the indole-*N*-alkyl chain [38], ether groups were introduced at this site of the molecule, and simultaneously, the influence of its length on the CB$_2$ binding affinity was investigated. Thus, the glycol ether compound **6** was synthesized from **3** by using 2-(2-(2-fluoroethoxy)ethoxy)ethyl-4-methylbenzenesulfonate [39,40] as alkylating reagent in 72% yield. Similarly, alcohol **4** was synthesized by reacting compound **3** with 2-bromethanol. Alcohol **4** was further etherified via Williamson ether synthesis [41] by using methyl iodide and 2-fluoro-1-bromoethane to give compounds **7** and **8**, respectively (for ^{1}H-NMR of compounds **3**, **5**, **6**, **7** and **8** see Supplementary Materials).

The binding affinity towards CB$_2$ receptors was determined in vitro by radioligand inhibition binding assays according to a recently published protocol [42,43] using cell membranes from CHO cells stably transfected with the human CB$_2$ (Prof Paul L. Prather, University Arkansas for Medical Sciences, Little Rock, AR, USA), [^{3}H]WIN55.212-2 as competitive radioligand (K_D = 2.1 nM) and increasing concentrations (100 pM to 10 μM) of compounds **5**, **6**, **7**, and **8** added in triplicate for each experiment. Non-specific binding was determined using 10 μM WIN55.212-2. The individual IC$_{50}$ values were determined by non-linear curve fitting using GraphPad Prism software (version 3.0, GraphPhad, San Diego, CA, USA), and the corresponding K_i values calculated using the Cheng–Prusoff equation [44]. As shown by the K_i values in Figure 1b, we could not reproduce the reported sub-nanomolar CB$_2$ affinity of the lead molecule (compound **5**) [32], but recorded a K_i value of 8.5 nM instead. In addition, these values and the individual binding curves in Figure 1a illustrate that a similar low-nanomolar affinity was observed for the fluorinated derivative **8** (K_i = 6.2 nM), while slightly lower affinities were determined for compounds **6** and **7** (K_i = 27.3 nM, and K_i = 16.1 nM, respectively). Additionally, the binding affinities towards the CB$_1$ receptor were investigated for compounds **6** and **8** by using [^{3}H]CP55.40 as competitive radioligand. None of the two derivatives could displace [^{3}H]CP55.40 from the human CB$_1$ receptors up to a concentration of 100 μM. Thus, within this series of fluoro-substituted compounds, the *N*-alkyl chain of compound **8** is most suitable to obtain high affinity binding at the CB$_2$ receptor, combined with an excellent selectivity against the CB$_1$ receptor subtype.

Cpd.	K_i [a] (CB$_2$) (nM)
5	8.5 ± 1.2 (0.37 [b])
6	27.3 ± 12
7	16.1 ± 6
8	6.2 ± 0.02

(a)   (b)
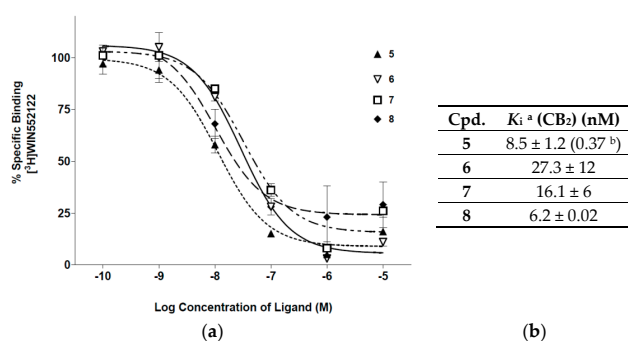
Figure 1. (**a**) Individual competition binding curves of compounds **5**, **6**, **7**, and **8**. Inhibition of [^{3}H]WIN55.212-2 binding by increasing concentrations (100 pM to 10 μM) of compounds **5**, **6**, **7**, and **8** to membrane homogenates of CHO cells stably transfected with human CB$_2$. Each value represents the mean ± standard deviation of a triplicate in a single experiment; (**b**) Binding affinity (K_i) of compounds **5**, **6**, **7**, and **8** for the human cannabinoid receptor type 2 (CB$_2$) receptor. [a] Values are means ± standard deviations of two to three experiments run in triplicate; [b] K_i of compound **5** as reported in [23].

3. Materials and Methods

3.1. General Methods

All reagents were used directly as obtained commercially, unless otherwise noted. Reaction progress was monitored by thin-layer chromatography (TLC) using silica gel 60 F254 (0.040–0.063 mm) with detection by UV. All moisture-sensitive reactions were performed under an argon atmosphere using oven-dried glassware and anhydrous solvents. Column flash chromatography was carried out using E. Merck silica gel 60F (230–400 mesh) (Merck Millipore, Darmstadt, Germany). Analytical TLC was performed on aluminum sheets coated with silica gel 60 F254 (0.25 mm thickness, E. Merck, Darmstadt, Germany). ^{1}H-NMR spectra were recorded with a Bruker-400 NMR spectrometer (Bruker, Billerica, MA, USA) at nominal resonance frequencies of 400 MHz, in $CDCl_3$ or DMSO-d_6 (referenced to internal Me_4Si at δH 0 ppm). The chemical shifts (δ) were expressed in parts per million (ppm). High resolution mass spectra were recorded utilizing electrospray ionization (ESI) at the University of Notre Dame Mass Spectrometry facility.

3.2. Procedures and Compound Characterization

N-(Adamantan-1-yl)-2-(5-(furan-2-yl)-1-(2-hydroxyethyl)-1H-indol-3-yl)-2-oxoacetamide (**4**). 2-bromethanol (55 μL, 1.2 eq, 0.77 mmol) was added to a solution of **3** (300 mg, 1 eq, 0.64 mmol) in 5 mL *N*,*N*-dimethylformamide (DMF) at room temperature, followed by powder KOH (116 mg, 3 eq, 1.93 mmol), and the reaction mixture was warmed to 90 °C for 6 h. Saturated aqueous $NaHCO_3$ solution (15 mL) and ethyl acetate (EA, 15 mL) were added, and the phases were separated. The aqueous phase was washed 2 × EA (10 mL), the combined organic solutions were dried over $MgSO_4$, filtered, and concentrated by rotary evaporation. The residue was purified by column chromatography (silica, EA:Hex, 1/1) to give alcohol **4** (224 mg, 67% yield) as yellow solid. ^{1}H-NMR (400 MHz, $CDCl_3$): δ (ppm) = 1.67–1.76 (m, 6H), 2.05–2.12 (m, 6H), 2.07–2.11 (m, 6H), 2.14 (br s, 3H), 2.41 (br s, 1H), 3.96–4.06 (t, *J* = 5.18 Hz, 2H), 4.31 (t, *J* = 5.18 Hz, 2H), 6.51 (dd, *J* = 3.28, 1.77 Hz, 1H), 6.71 (dd, *J* = 3.28, 0.76 Hz, 1H), 7.35 (s, 1H), 7.40 (dd, *J* = 8.59, 0.76 Hz, 1H), 7.50 (dd, *J* = 1.77, 0.76 Hz, 1H), 7.65 (dd, *J* = 8.59, 1.52 Hz, 1H), 8.71 (dd, *J* = 1.77, 0.51 Hz, 1H), 8.99–9.10 (m, 1H). ^{13}C-NMR (100 MHz, $CDCl_3$): δ (ppm) = 29.36 (3C), 36.29 (3C), 41.15 (3C), 49.58, 51.84, 61.26, 104.42, 110.40, 111.72, 112.16, 118.02, 120.29, 126.77, 128.24, 135.74, 141.77, 142.03, 154.59, 161.48, 181.14.

N-(Adamantan-1-yl)-2-(5-(furan-2-yl)-1-pentyl-1H-indol-3-yl)-2-oxoacetamide (**5**). This compound was obtained according to literature. ^{1}H-NMR (400 MHz, $CDCl_3$): δ (ppm) = 0.86–0.94 (m, 3H), 1.28–1.44 (m, 4H), 1.69–1.81 (m, 6H), 1.93 (quin, *J* = 7.33 Hz, 2H), 2.10–2.20 (m, 9H), 4.16 (t, *J* = 7.33 Hz, 2H), 6.51 (dd, *J* = 3.28, 1.77 Hz, 1H), 6.73 (dd, *J* = 3.28, 0.76 Hz, 1H), 7.37–7.44 (m, 2 H), 7.50 (dd, *J* = 1.89, 0.63 Hz, 1H), 7.69 (dd, *J* = 8.59, 1.77 Hz, 1H), 8.73–8.78 (m, 1H), 9.04 (s, 1H). ^{13}C-NMR (100 MHz, $CDCl_3$): δ (ppm) = 13.94, 22.29, 28.99, 29.38 (3C), 29.60, 36.32 (3C), 41.21 (3C), 47.58, 51.78, 104.35, 110.43, 111.70, 111.91, 118.10, 120.13, 126.67, 128.36, 135.60, 141.62, 141.74, 154.70, 161.58, 180.97.

N-(Adamantan-1-yl)-2-(1-(2-(2-(2-fluoroethoxy)ethoxy)ethyl)-5-(furan-2-yl)-1H-indol-3-yl)-2-oxoacetamide (**6**). 2-(2-(2-fluoroethoxy)ethoxy)ethyl-4-methylbenzenesulfonate (40 mg, 1.5 eq, 0.15 mmol) and KOH (25 mg, 5 eq, 0.5 mmol) were added at room temperature to a solution of compound **3** (46 mg, 1 eq, 0.1 mmol) in 3 mL DMF, and the reaction mixture was warmed to 90 °C for 6 h. To the cooled down solution, 15 mL saturated aqueous $NaHCO_3$ solution was added followed by 15 mL EA. The phases were separated, and the aqueous phase was separated 2 × 10 mL EA. The combined organic phases were washed with 20 mL brine, dried over $MgSO_4$, and concentrated under reduced pressure. The resulting residue was purified by column chromatography (silica, EA:Hex, 1/1) to give **6** (44 mg, 72% yield) as yellow solid. ^{1}H-NMR (400 MHz, $CDCl_3$): δ (ppm) = 1.68–1.79 (m, 6H), 2.08–2.19 (m, 9H), 3.51–3.71 (m, 6H), 3.65–3.70 (m, 2H), 3.90 (t, *J* = 5.43 Hz, 2H), 4.37 (t, *J* = 5.43 Hz, 2H), 4.40–4.45 (m, 1H), 4.49–4.68 (m, 1 H), 6.51 (dd, *J* = 3.28, 1.77 Hz, 1H), 6.72 (dd, *J* = 3.28, 0.76 Hz, 1H), 7.38 (s, 1H), 7.41–7.54 (m, 2H), 7.69 (dd, *J* = 8.59, 1.77 Hz, 1H), 8.69–8.88 (m, 1H), 9.08 (s, 1H). ^{13}C-NMR (100 MHz,

CDCl$_3$): δ (ppm) = 29.38 (3C), 36.32 (3C), 41.20 (3C), 47.43, 51.76, 69.66 (2C), 70.43, 70.62, 70.81, 71.02 (2C), 83.95, 104.37, 110.64, 111.70, 117.98, 120.15, 126.69, 128.21, 135.84, 141.76, 142.29, 181.21. HRMS (ESI+): *m/z* (%) = 523.6150 (ccd. 523.6151) [M + H]$^+$.

N-(Adamantan-1-yl)-2-(5-(furan-2-yl)-1-(2-methoxyethyl)-1H-indol-3-yl)-2-oxoacetamide (**7**). NaH (60% suspension in mineral oil, 10 mg, 2 eq, 0.25 mmol) was added to a solution of **4** (65 mg, 1 eq, 1.12 mmol) in 2 mL DMF at 0 °C, and the mixture was stirred at 0 °C for 15 min. MeI (64 μL, 8 eq, 1.02 mmol) was added, the ice bath was removed, and the reaction was magnetically stirred at room temperature. After 5 h, the reaction was quenched by slow addition of 2 mL cold water followed by 10 mL saturated aqueous NaHCO$_3$ solution and 15 mL EA. The phases were separated, and the aqueous phase was washed three times with 10 mL EA. The combined organic phases were washed with brine, dried over MgSO$_4$, and concentrated under reduced pressure. The resulting material was purified by column chromatography (silica, EA:Hex, 1/1) to give **7** (55 mg, 84% yield), yellow solid. ^{1}H-NMR (400 MHz, CDCl$_3$): δ (ppm) = 1.75 (m., 6H), 2.10–2.20 (m, 9H), 3.25–3.39 (s, 3H), 3.77 (t, *J* = 5.43 Hz, 2H), 4.34 (t, *J* = 5.43 Hz, 2H), 6.46–6.55 (m, 1H), 6.68–6.78 (m, 1H), 7.39 (s, 1H), 7.40–7.45 (m, 1H), 7.47–7.54 (m, 1H), 7.69 (dd, *J* = 8.59, 1.77 Hz, 1H), 8.74 (d, *J* = 1.77 Hz, 1H), 9.01–9.10 (m, 1H). ^{13}C-NMR (100 MHz, CDCl$_3$): δ (ppm) = 30.00 (3C), 31.81, 36.43 (3C), 39.23 (3C), 47.15, 59.15, 70.73, 104.46, 110.37, 111.71, 120.26, 138.52, 141.71, 161.32, 181.22. HRMS (ESI+): *m/z* (%) = 447.5457 (ccd. 447.5455) [M + H]$^+$.

N-(Adamantan-1-yl)-2-(1-(2-(2-fluoroethoxy)ethyl)-5-(furan-2-yl)-1H-indol-3-yl)-2-oxoacetamide (**8**). This compound was synthesized by employing the same procedure as for compound **7**, and it was obtained in 75% yield as yellow solid. ^{1}H-NMR (400 MHz, CDCl$_3$): δ (ppm) = 1.75 (m, 6H), 2.07–2.21 (m, 9H), 3.58–3.66 (m, 1H), 3.66–3.72 (m, 1H), 3.92 (t, *J* = 5.56 Hz, 2H), 4.38 (t, *J* = 5.43 Hz, 2H), 4.42–4.48 (m, 1H), 4.52–4.60 (m, 1H), 6.46–6.55 (m, 1H), 6.73 (dd, *J* = 3.28, 0.76 Hz, 1H), 7.37 (s, 1H), 7.46 (dd, *J* = 8.59, 0.51 Hz, 1H), 7.50 (dd, *J* = 1.77, 0.76 Hz, 1H), 7.70 (dd, *J* = 8.59, 1.77 Hz, 1H), 8.75 (dd, *J* = 1.64, 0.63 Hz, 1H), 9.07 (s, 1H). ^{13}C-NMR (100 MHz, CDCl$_3$): δ (ppm) = 29.38 (3C), 36.32 (3C), 41.20 (3C), 47.44, 51.79, 69.88, 70.47, 70.67, 82.31, 83.99, 104.39, 110.59, 111.70, 112.25, 118.00, 120.23, 128.21, 135.82, 141.76, 142.14, 154.65, 161.45. HRMS (ESI+): *m/z* (%) = 479.5627 (ccd. 479.5625) [M + H]$^+$.

4. Conclusions

In this study, the *N*-alkyl chain of the high affinity and selective CB$_2$ ligand **5** was modified for the possibility of introducing a fluorine atom. The herein developed fluorinated compound **8** retained the high affinity of the lead compound, and will be considered for the development of an ^{18}F-labeled radiotracer for CB$_2$ receptors imaging with PET.

Author Contributions: Rareş-Petru Moldovan and Andrew G. Horti conceived and performed the chemical syntheses. Winnie Deuther-Conrad and Peter Brust planned and performed the radioligand binding studies.

Abbreviations

CB$_2$	cannabinoid receptors type 2
CB$_1$	cannabinoid receptors type 1
PET	positron emission tomography
DMF	*N,N*-dimethylformamide
TBAB	tetrabutylammonium bromide
Et$_3$N	triethylamine
CHO	Chinese Hamster Ovary
EA	ethyl acetate
Et$_2$O	diethyl ether
DCM	dichloromethane
Pd(PPh$_3$)$_4$	tetrakis(triphenylphosphine)palladium(0)
n-BuBr	1-bromobutane
MeI	methyl iodide
Hex	hexane

References and Notes

1. Gaoni, Y.; Mechoulam, R. Isolation structure and partial synthesis of active constituent of hashish. *J. Am. Chem. Soc.* **1964**, *86*, 1646–1647. [CrossRef]

2. Piomelli, D. The molecular logic of endocannabinoid signalling. *Nat. Rev. Neurosci.* **2003**, *4*, 873–884. [CrossRef] [PubMed]

3. Schlicker, E.; Kathmann, M. Modulation of transmitter release via presynaptic cannabinoid receptors. *Trends Pharmacol. Sci.* **2001**, *22*, 565–572. [CrossRef]

4. Matsuda, L.A.; Lolait, S.J.; Brownstein, M.J.; Young, A.C.; Bonner, T.I. Structure of a cannabinoid receptor and functional expression of the cloned cDNA. *Nature* **1990**, *346*, 561–564. [CrossRef] [PubMed]

5. Munro, S.; Thomas, K.L.; Abu-Shaar, M. Molecular characterization of a peripheral receptor for cannabinoids. *Nature* **1993**, *365*, 61–65. [CrossRef] [PubMed]

6. Hillard, C.J. The endocannabinoid signaling system in the CNS: A primer. *Int. Rev. Neurobiol.* **2015**, *125*, 1–47. [PubMed]

7. Hua, T.; Vemuri, K.; Pu, M.; Qu, L.; Han, G.W.; Wu, Y.; Zhao, S.; Shui, W.; Li, S.; Korde, A.; et al. Crystal structure of the human cannabinoid receptor CB$_1$. *Cell* **2016**, *167*, 750–762. [CrossRef] [PubMed]

8. Shao, Z.; Yin, J.; Chapman, K.; Grzemska, M.; Clark, L.; Wang, J.; Rosenbaum, D.M. High-resolution crystal structure of the human CB$_1$ cannabinoid receptor. *Nature* **2016**. [CrossRef] [PubMed]

9. Howlett, A.C.; Barth, F.; Bonner, T.I.; Cabral, G.; Casellas, P.; Devane, W.A.; Felder, C.C.; Herkenham, M.; Mackie, K.; Martin, B.R.; et al. International Union of Pharmacology. XXVII. Classification of cannabinoid receptors. *Pharmacol. Rev.* **2002**, *54*, 161–202. [CrossRef] [PubMed]

10. Cabral, G.A.; Ferreira, G.A.; Jamerson, M.J. Endocannabinoids and the immune system in health and disease. *Handb. Exp. Pharmacol.* **2015**, *231*, 185–211. [PubMed]

11. Stella, N. Cannabinoid signaling in glial cells. *Glia* **2004**, *48*, 267–277. [CrossRef] [PubMed]

12. Palazuelos, J.; Aguado, T.; Egia, A.; Mechoulam, R.; Guzman, M.; Galve-Roperh, I. Non-psychoactive CB$_2$ cannabinoid agonists stimulate neural progenitor proliferation. *FASEB J.* **2006**, *20*, 2405–2407. [CrossRef] [PubMed]

13. Molina-Holgado, E.; Vela, J.M.; Arevalo-Martin, A.; Almazan, G.; Molina-Holgado, F.; Borrell, J.; Guaza, C. Cannabinoids promote oligodendrocyte progenitor survival: Involvement of cannabinoid receptors and phosphatidylinositol-3 kinase/Akt signaling. *J. Neurosci.* **2002**, *22*, 9742–9753. [PubMed]

14. Maresz, K.; Carrier, E.J.; Ponomarev, E.D.; Hillard, C.J.; Dittel, B.N. Modulation of the cannabinoid CB$_2$ receptor in microglial cells in response to inflammatory stimuli. *J. Neurochem.* **2005**, *95*, 437–445. [CrossRef] [PubMed]

15. Li, Y.; Kim, J. Neuronal expression of CB$_2$ cannabinoid receptor mRNAs in the mouse hippocampus. *Neuroscience* **2015**, *311*, 253–267. [CrossRef] [PubMed]

16. Wolfson, M.L.; Muzzio, D.O.; Ehrhardt, J.; Franchi, A.M.; Zygmunt, M.; Jensen, F. Expression analysis of cannabinoid receptors 1 and 2 in B cells during pregnancy and their role on cytokine production. *J. Reprod. Immunol.* **2016**, *116*, 23–27. [CrossRef] [PubMed]

17. Eisenstein, T.K.; Meissler, J.J. Effects of cannabinoids on T-cell function and resistance to infection. *J. Neuroimmune Pharmacol.* **2015**, *10*, 204–216. [CrossRef] [PubMed]

18. Bisogno, T.; Oddi, S.; Piccoli, A.; Fazio, D.; Maccarrone, M. Type-2 cannabinoid receptors in neurodegeneration. *Pharmacol. Res.* **2016**, *111*, 721–730. [CrossRef] [PubMed]

19. Ashton, J.C.; Glass, M. The cannabinoid CB_2 receptor as a target for inflammation-dependent neurodegeneration. *Curr. Neuropharmacol.* **2007**, *5*, 73–80. [CrossRef] [PubMed]

20. Turcotte, C.; Blanchet, M.R.; Laviolette, M.; Flamand, N. The CB_2 receptor and its role as a regulator of inflammation. *Cell. Mol. Life Sci.* **2016**, *73*, 4449–4470. [CrossRef] [PubMed]

21. Benito, C.; Romero, J.P.; Tolon, R.M.; Clemente, D.; Docagne, F.; Hillard, C.J.; Guaza, C.; Romero, J. Cannabinoid CB_1 and CB_2 receptors and fatty acid amide hydrolase are specific markers of plaque cell subtypes in human multiple sclerosis. *J. Neurosci.* **2007**, *27*, 2396–2402. [CrossRef] [PubMed]

22. Sanchez, C.; de Ceballos, M.L.; Gomez del Pulgar, T.; Rueda, D.; Corbacho, C.; Velasco, G.; Galve-Roperh, I.; Huffman, J.W.; Ramon y Cajal, S.; Guzman, M. Inhibition of glioma growth in vivo by selective activation of the CB_2 cannabinoid receptor. *Cancer Res.* **2001**, *61*, 5784–5789. [PubMed]

23. Fernandez-Ruiz, J.; Romero, J.; Ramos, J.A. Endocannabinoids and neurodegenerative disorders: Parkinson's Disease, Huntington's Chorea, Alzheimer's Disease, and others. *Handb. Exp. Pharmacol.* **2015**, *231*, 233–259. [PubMed]

24. Aizpurua-Olaizola, O.; Elezgarai, I.; Rico-Barrio, I.; Zarandona, I.; Etxebarria, N.; Usobiaga, A. Targeting the endocannabinoid system: Future therapeutic strategies. *Drug. Discov. Today* **2016**. [CrossRef] [PubMed]

25. Brust, P.; van den Hoff, J.; Steinbach, J. Development of [^{18}F]-labeled radiotracers for neuroreceptor imaging with positron emission tomography. *Neurosci. Bull.* **2014**, *30*, 777–811. [CrossRef]

26. Horti, A.G.; Raymont, V.; Terry, G.E. PET imaging of endocannabinoid system. In *PET and SPECT of Neurobiological Systems*; Dierckx, R.A.J.O., Otte, A., de Vries, E.F.J., van Waarde, A., Luiten, P.G.M., Eds.; Springer: Berlin. Germany, 2014; pp. 249–319.

27. Evens, N.; Bormans, G.M. Non-invasive imaging of the type 2 cannabinoid receptor, focus on positron emission tomography. *Curr. Top. Med. Chem.* **2010**, *10*, 1527–1543. [CrossRef]

28. Ory, D.; Celen, S.; Verbruggen, A.; Bormans, G. PET radioligands for in vivo visualization of neuroinflammation. *Curr. Pharm. Des.* **2014**, *20*, 5897–5913. [CrossRef]

29. (a) Ahmad, R.; Postnov, A.; Bormans, G.; Versijpt, J.; Vandenbulcke, M.; van Laere, K. Decreased in vivo availability of the cannabinoid type 2 receptor in Alzheimer's disease. *E. J. Nucl. Med. Mol. Imaging* **2016**, 1–9; (b) Slavik, R.; Muller Herde, A.; Haider, A.; Kramer, S. D.; Weber, M.; Schibli, R.; Ametamey, S.M.; Mu, L. Discovery of a fluorinated 4-oxo-quinoline derivative as a potential positron emission tomography radiotracer for imaging cannabinoid receptor type 2. *J. Neurochem.* **2016**, 874–886; (c) Haider, A.; Müller Herde, A.; Slavik, R.; Weber, M.; Mugnaini, C.; Ligresti, A.; Schibli, R.; Mu, L.; Mensah Ametamey, S. Synthesis and Biological Evaluation of Thiophene-Based Cannabinoid Receptor Type 2 Radiotracers for PET Imaging. *Front. Neurosci.* **2016**, 10:350; (d) Slavik, R.; Herde, A.M.; Bieri, D.; Weber, M.; Schibli, R.; Kramer, S.D.; Ametamey, S. M.; Mu, L. Synthesis, radiolabeling and evaluation of novel 4-oxo-quinoline derivatives as PET tracers for imaging cannabinoid type 2 receptor. *Eur. J. Med. Chem.* **2015**, *92c*, 554–564.

30. D'Ambra, T.E.; Estep, K.G.; Bell, M.R.; Eissenstat, M.A.; Josef, K.A.; Ward, S.J.; Haycock, D.A.; Baizman, E.R.; Casiano, F.M. Conformationally restrained analogs of pravadoline: Nanomolar potent, enantioselective, (aminoalkyl)indole agonists of the cannabinoid receptor. *J. Med. Chem.* **1992**, *35*, 124–135. [CrossRef]

31. Eissenstat, M.A.; Bell, M.R.; D'Ambra, T.E.; Alexander, E.J.; Daum, S.J.; Ackerman, J.H.; Gruett, M.D.; Kumar, V.; Estep, K.G. Aminoalkylindoles: Structure-activity relationships of novel cannabinoid mimetics. *J. Med. Chem.* **1995**, *38*, 3094–3105. [CrossRef]

32. Pasquini, S.; Mugnaini, C.; Ligresti, A.; Tafi, A.; Brogi, S.; Falciani, C.; Pedani, V.; Pesco, N.; Guida, F.; Luongo, L.; et al. Design, synthesis, and pharmacological characterization of indol-3-ylacetamides, indol-3-yloxoacetamides, and indol-3-ylcarboxamides: Potent and selective CB_2 cannabinoid receptor inverse agonists. *J. Med. Chem.* **2012**, *55*, 5391–5402. [CrossRef]

33. Aung, M.M.; Griffin, G.; Huffman, J.W.; Wu, M.-J.; Keel, C.; Yang, B.; Showalter, V.M.; Abood, M.E.; Martin, B.R. Influence of the *N*-1 alkyl chain length of cannabimimetic indoles upon CB_1 and CB_2 receptor binding. *Drug Alcohol Depend.* **2000**, *60*, 133–140. [CrossRef]

34. Lipinski, C.A. Drug-like properties and the causes of poor solubility and poor permeability. *J. Pharmacol. Toxicol. Methods* **2000**, *44*, 235–249. [CrossRef]

35. (a) Moldovan, R.-P.; Teodoro, R.; Gao, Y.; Deuther-Conrad, W.; Kranz, M.; Wang, Y.; Kuwabara, H.; Nakano, M.; Valentine, H.; Fischer, S.; et al. Development of a high-affinity PET radioligand for imaging cannabinoid subtype 2 receptor. *J. Med. Chem.* **2016**, *59*, 7840–7855; (b) Savonenko, A.V.; Melnikova, T.; Wang, Y.; Ravert, H.; Gao, Y.; Koppel, J.; Lee, D.; Pletnikova, O.; Cho, E.; Sayyida, N.; et al. Cannabinoid CB_2 receptors in a mouse model of $A\beta$ amyloidosis: immunohistochemical analysis and suitability as a PET biomarker of neuroinflammation. *PLoS ONE* **2015**, *10*, e0129618; (c) Horti, A.G.; Gao, Y.; Ravert, H.T.; Finley, P.; Valentine, H.; Wong, D.F.; Endres, C.J.; Savonenko, A.V.; Dannals, R.F. Synthesis and biodistribution of [^{11}C]A-836339, a new potential radioligand for PET imaging of cannabinoid type 2 receptors (CB_2). *Bioorg. Med. Chem.* **2010**, *18*, 5202–5207.

36. Pasquini, S.; Mugnaini, C.; Brizzi, A.; Ligresti, A.; di Marzo, V.; Ghiron, C.; Corelli, F. Rapid Combinatorial Access to a Library of 1,5-Disubstituted-3-indole-*N*-alkylacetamides as CB_2 Receptor Ligands. *J. Comb. Chem.* **2009**, *11*, 795–798. [CrossRef] [PubMed]

37. Pasquini, S.; Ligresti, A.; Mugnaini, C.; Semeraro, T.; Cicione, L.; de Rosa, M.; Guida, F.; Luongo, L.; de Chiaro, M.; Cascio, M.G.; et al. Investigations on the 4-quinolone-3-carboxylic acid motif. 3. Synthesis, structure-affinity relationships, and pharmacological characterization of 6-substituted 4-quinolone-3-carboxamides as highly selective cannabinoid-2 receptor ligands. *J. Med. Chem.* **2010**, *53*, 5915–5928. [CrossRef] [PubMed]

38. Mugnaini, C.; Brizzi, A.; Ligresti, A.; Allarà, M.; Lamponi, S.; Vacondio, F.; Silva, C.; Mor, M.; di Marzo, V.; Corelli, F. Investigations on the 4-Quinolone-3-carboxylic Acid Motif. 7. Synthesis and Pharmacological Evaluation of 4-Quinolone-3-carboxamides and 4-Hydroxy-2-quinolone-3-carboxamides as High Affinity Cannabinoid Receptor 2 (CB2R) Ligands with Improved Aqueous Solubility. *J. Med. Chem.* **2016**, *59*, 1052–1067. [PubMed]

39. Friscourt, F.; Fahrni, C.J.; Boons, G.-J. A fluorogenic probe for the catalyst-free detection of azide-tagged molecules. *J. Am. Chem. Soc.* **2012**, *134*, 18809–18815. [CrossRef] [PubMed]

40. Cui, M.; Wang, X.; Yu, P.; Zhang, J.; Li, Z.; Zhang, X.; Yang, Y.; Ono, M.; Jia, H.; Saji, H.; et al. Synthesis and evaluation of novel ^{18}F labeled 2-pyridinylbenzoxazole and 2-pyridinylbenzothiazole derivatives as ligands for positron emission tomography (PET) imaging of β-amyloid plaques. *J. Med. Chem.* **2012**, *55*, 9283–9296. [CrossRef] [PubMed]

41. Williamson, A. XLV. Theory of aetherification. *Philos. Mag. Ser.* **1850**, *37*, 350–356.

42. Rühl, T.; Deuther-Conrad, W.; Fischer, S.; Günther, R.; Hennig, L.; Krautscheid, H.; Brust, P. Cannabinoid receptor type 2 (CB_2)-selective *N*-aryl-oxadiazolyl-propionamides: Synthesis, radiolabelling, molecular modelling and biological evaluation. *Org. Med. Chem. Lett.* **2012**, *2*, 32. [CrossRef] [PubMed]

43. Teodoro, R.; Moldovan, R.-P.; Lueg, C.; Günther, R.; Donat, C.K.; Ludwig, F.-A.; Fischer, S.; Deuther-Conrad, W.; Wünsch, B.; Brust, P. Radiofluorination and biological evaluation of *N*-aryl-oxadiazolyl-propionamides as potential radioligands for PET imaging of cannabinoid CB_2 receptors. *Org. Med. Chem. Lett.* **2013**, *3*, 1–18. [CrossRef] [PubMed]

44. Yung-Chi, C.; Prusoff, W.H. Relationship between the inhibition constant (K_I) and the concentration of inhibitor which causes 50 per cent inhibition (I_{50}) of an enzymatic reaction. *Biochem. Pharmacol.* **1973**, *22*, 3099–3108.